LRP 764/03 May 2003

In-Beam Mechanical Testing of CuCrZr

(EFDA Task TW1-TVV/Beam)

P. Marmy

ISSN 0458-5895

EFDA TASK TW1-TVV/Beam

In-Beam Mechanical Testing of CuCrZr

by Pierre Marmy

Centre de Recherche en Physique des Plasmas,
Technologie de la fusion
Association Euratom- Confédération Suisse
Ecole Polytechnique fédérale de Lausanne
5232 Villigen , PSI, Switzerland

Summary:

1. Introduction

In the ITER design, a high thermal conductivity material, a copper alloy , is interposed between the materials facing the plasma and the cooling water channels structure. The main role of the copper interlayer is to transport the heat deposited in the armour materials to the cooling water channel structure. The temperature gradient associated with the large heat flux will induce thermal stresses in the copper components. Due to the pulse operation of the tokamak, those stresses will be cyclic in nature. They will act on the copper alloy being at the same time irradiated with a flux of high energy neutrons. A maximum number of pulses of 30,000 with a duration of up to 400 sec will be imposed on the components. At the first wall, the dose in dpa will reach up to 3 dpa and the temperature will lie between 100 and approximately 300°C, whereas at the divertor, dose and temperature will reach respectively 0.3 dpa and 400 °C.
Due to a good combination of physical and mechanical properties, among them a better fracture toughness and relatively good irradiation resistance, CuCrZr seems to be the most adequate material for the copper interlayer in ITER [1].
Thermo-mechanical stresses not far from the yield point will be induced in the components and cyclic plastic strains may be produced at stress concentrations [2]. For this reason, the low cycle fatigue performance has been studied extensively in the past for the copper alloys candidate materials (CuCrZr,CuAl25,CuNiCr). The fatigue behaviour has been measured before and after the irradiation with fission neutrons, at temperatures between 22 and 350°C.
For the CuCrZr alloy in particular, the results obtained seem to indicate a fatigue behavior close to the one observed in OFHC Cu, from the point of view of the mechanical properties and the dislocation structures developed after deformation [3]. When compared to CuNiBe or CuAl25 (Glidcop) the fatigue performance is slightly inferior. When tested under stress control, the neutron irradiated material at 100°C exhibits sharp yield points in contrary to the Glidcop alloy which shows none [4]. This problem has been also described after tensile tests at moderate temperatures and causes a strong reduction of the uniform strain in the case of irradiated CuCrZr alloy and OFHC copper [5], in particular after irradiations with neutrons and test temperatures around 47°C. After irradiation to higher temperatures (T=250°C), there is no strain instability problem anymore [6] . Therefore it was decided to conduct the first in-situ testing of CuCrZr around 100°C, where the material still seems to suffer strongly from strain instabilities.
The test program includes three basic tests, all performed at 100°C and at a strain amplitude of 0.8%, an unirradiated fatigue test performed with the *in-situ* device, the *in-beam* test and the *post-irradiation* comparison fatigue test.

2. Origin and chemical analysis of the CuCrZr alloy

The material used in this study is a precipitation hardened copper alloy produced by the company Otokumpu in Finland. The chemical composition of this alloy is given in Table 1. The material was delivered in the form of a plate of 46 mm thickness. The plate had been previously cold rolled about 60% after solution anneal at 960°C for 1 h and subsequently precipitation heat treated at 460°C for 2 h.

Table 1: Chemical composition of CuCrZr in wt%

Designation	Cr	Zr	Si	Cu
CuCrZr	0.78	0.13	0.003	Rest

3. Applied Heat Treatment and related microstructure

Four cylinders having 20 mm in diameter and 120 mm in length have been cut from the plate in the longitudinal direction, by electro-erosion. The expected crack plane orientation is L-S or L-T, assuming the crack would propagate in a plane normal to specimen axis. One additional specimen with similar dimensions has been machined and reserved for microstructural examinations. The heat treatments were done into a vacuum oven at 10^{-3} mbar. The quench was done by filling nitrogen in the vacuum chamber and immediate immersion of the specimen into water. The whole operation was executed in less than 10 seconds. The following heat treatment consisting of a solution anneal and precipitation heating, was given to the specimens:

30 min at 975 °C, water quench, 30 min at 475 °C, water quench

A series of hardness measurements was conducted on the machined cylinders, before and after the heat treatments, in order to follow the microstructural changes. Results are indicated in Table 2.

Table 2: Vickers hardness HV30 according to DIN 50133, before and after the heat treatment

As received	115	114	115
Heat treated	136	134	132

After the above heat treatments, a bimodal distribution of mesoscopic and microscopic precipitates is observed in the material. The mesoscopic precipitates have sizes between 0.1 and 1 μm and spacing of 5-10 μm. The microscopic fine precipitates have a size of 2-10 nm (mean size around 3 nm) and spacings of 30-40 nm. The coarse precipitates resist most thermal treatments and have no significant effect on physical and mechanical properties. The fine precipitates were identified to consist of two different types having the same number density, Guinier-Preston coherent precipitates and incoherent fringed precipitates [6]. An EDX analysis performed by Holzwarth et al. [7] indicates that the precipitates are Zr enriched. The fine precipitation controls the mechanical properties of the alloy. The grain size resulting from the above heat treatment (prime ageing) should lie around 27 μm [8].

4. Description of experiment

4.1 In-Situ Device

In beam fatigue tests are conducted with the *in-situ* device, a specially dedicated irradiation head of the PIREX facility [9], at the PSI accelerator. The irradiating particle used in the PIREX facility are 590 MeV protons. They deposit a large amount of heat in the materials, which has to be removed by forced cooling. A flow of pressurized helium (30 bars, 100 Nm^3/h) is used for cooling the irradiated specimen.

The *in-situ* device consists of three subsystems: the vertical drive which moves the machine *in* and *out of beam*, the helium temperature controlling system consisting of an heat recuperator and a heater and finally the testing machine on the bottom of the system. The *in-situ* device is shown in Figure 1, in the extended configuration.

The specimen is mounted between the grips, at the bottom of the system.
The *in-situ* device is installed in a container and the irradiation is performed under vacuum. After the experiment, the device is transported to the hot cells in a shielded transport bottle. More details on the machine are given in [10].

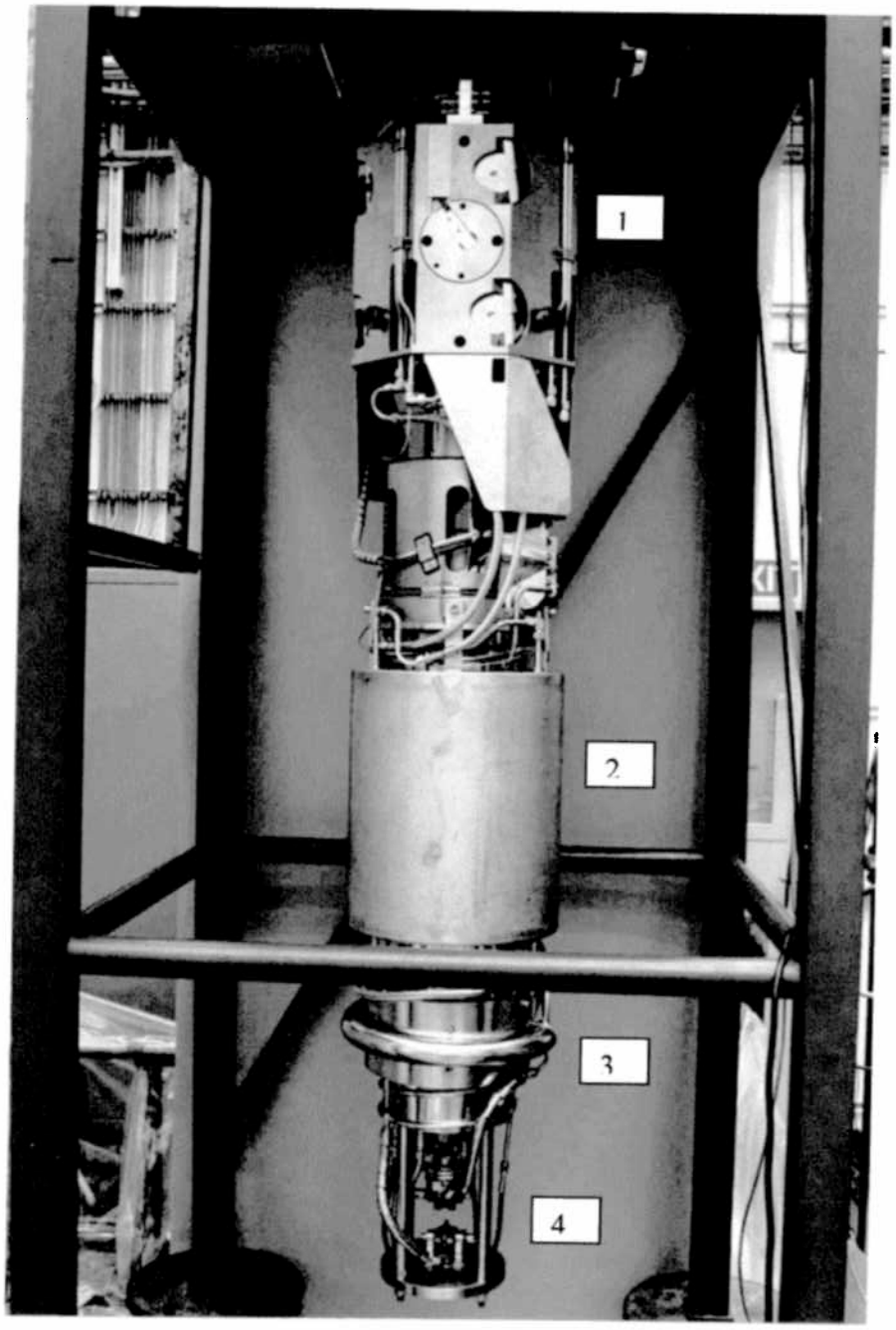

Figure 1: *Photograph of the in-situ device with its main components, the vertical drive which moves the system up and down 200mm (1), the heat recuperator (2), the heater which heats the helium up to 400°C (3), the grips of the testing machine with helium manifolds (4). The testing machine itself is located behind the recuperator and heater and is protected from the heat by a water cooled shield.*

4.2 Test Specimen

The test specimen is shown in Figure 2. It is a tubular specimen with an inside diameter of 2.5 mm and 0.45 mm wall thickness. The geometrical gauge length is 5 mm. During testing, helium at 100 Nm3/h and 30 bars, flows in the inside to extract the heat deposited by the protons. The outside of the specimen is in a vacuum at 2x10-2 mbar. Two thermocouples are glued on the copper material, in the center and at the end of the gauge length. The thermocouples are needed for adjusting the irradiation temperature and help for centering the beam. The specimen is sealed with two metallic O-rings. The failure under fatigue is indicated when the pressure in the surrounding vacuum increases. The test is then automatically interrupted.
The strain is measured with a mini strain extensometer applied onto the gauge length. The displacement is taken with two ceramic bars and transformed into an electrical output with a classical strain gage transducer. The effective gauge length, the length between the ceramic bars, is set to about 6 mm.

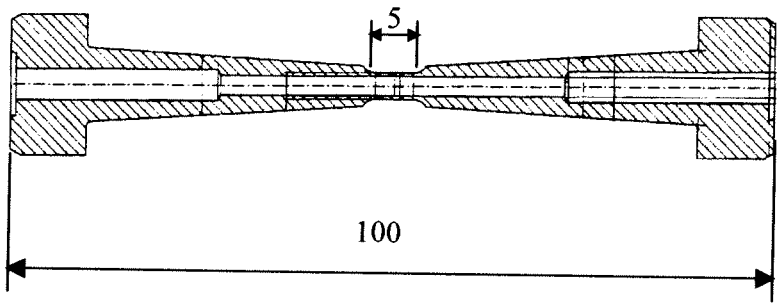

Figure 2: *The in situ specimen*

4.3 Beam Parameters and Mechanical Tests Details

The proton beam has a gaussian distribution. It was adjusted to a size of $4\sigma_y$=3 mm and $4\sigma_x$=6 mm. The beam was then wobbled with an amplitude of 2.5 mm along the gauge length, with a frequency of about 1.8 Hz, to achieve a constant dose distribution. The beam intensity was 11 μA. Under these conditions, the mean current density was 50 μA/cm^2 and the mean proton flux was 3x10^{14} p/cm^2/s.
The damage rate can then be evaluated from a modified Kinchin-Pease model:

$$\frac{dpa}{s} = \dot{D} = \frac{0.8 \cdot \Phi \cdot \delta_{E_D}}{2 \cdot E_T}$$

where Φ is the proton flux, δ_{Ed} is the calculated damage energy cross section (316 barn keV from[11]) and E_T the displacement threshold energy (25 eV from [11, 12]). The value obtained for $\dot{D}$ is 1.5 10^{-6} dpa/s. The 590 MeV protons also generate helium and hydrogen in the irradiated alloy. The calculated values for pure copper are respectively 126 and 530 appm/dpa [9, 11]. The irradiation parameters relevant for the irradiations are given in Table 3. The indicated dose is an estimation from the integration of the beam current.
The fatigue was conducted under total strain control, following a R=-1 triangular waveform signal. The total strain amplitude was 0.8 % (half strain amplitude 0.4%). The test frequency was chosen at 0.01 Hz (T=100 s) for the *in beam* test and 0.028 Hz (T=36 s) for the comparison tests. At 100°C, the test frequency should have no influence on the mechanical behavior, therefore, for practical reasons, the test frequency was reduced for the comparison tests.
During all mechanical tests, a test temperature of 100°C was adjusted onto the specimen, taking into account beam heating (see Fig. 4). Since spot welds are not possible on copper, the thermocouples were glued on the gauge length. Under irradiation, they would not survive more than a few hours. Therefore the temperature was adjusted at the beginning of the experiment and then all gas cooling and beam parameters were kept constant up to the end of the experiment.

The end of life criteria used to compare the lives was when the main crack penetrated through the specimen wall ($N=N_a$). This point was clearly indicated in the *in-beam* experiment by a failure of the vacuum produced by the out flowing helium. To this point corresponded an inflexion point in the bottom part of the strain-stress hysteresis, which is also clearly marked in the classical fatigue specimen, although no helium pressure is present in the specimen. After the test was interrupted by the vacuum failure, the test was continued without helium, in a vacuum, at an equilibrium temperature of about 40°C. N_a is considered a better parameter for comparison since at cycles higher than N_a, the mechanical conditions are modified. Depending on the orientation of the main crack, the number of cycles to failure is also affected by a larger dispersion.

The mechanical parameters of the fatigue test are given in Table 4.

Table 3: *The irradiation parameters estimated for the 590 MeV proton irradiation. N32I01 was tested in the facility without beam. I32I02 was in-beam tested. I32I04 was tested after irradiation. Predicted helium production ratio: 126 appm/dpa [9].*

	N32I01	I32I02	I32I04
Dose rate: $\dot{D}$ [dpa/s]	-	1.5×10^{-6}	1.5×10^{-6}
Damage ratio: $\dot{D}/\dot{\varepsilon}$ [dpa]	-	9.4×10^{-3}	5.5×10^{-3} 11.5×10^{-3} 25×10^{-3}
Accumulated dose: D [A.s]	-	2.453	1.521
Accumulated dose: D [dpa]	-	0.334	0.211

Table 4: *The mechanical tests parameters imposed to the specimens. The temperature was 100°C in all tests. Specimen N32I01 has been tested in the unirradiated condition. Specimen I32I02 was in-beam tested and specimen I32I04 was tested after irradiation. The damage ratios indicated for I32I04 are for the preliminary test.*

	N32I01	I32I02	I32I04
$\Delta\varepsilon$ tot[%]	0.8	0.8	0.8
T [sec]	36	100	36
$\dot{\varepsilon}$ [sec^{-1}]	4.44×10^{-4}	1.6×10^{-4}	4.44×10^{-4}

5. History of the three experiments

Before comparing the different results coming from the three experiments, it is necessary to present them in all details, in order to have a clear view on the content of those experiments and also to understand the limits of their use.

The first experiment realized was I32I01 which was conducted without beam, but using exactly the same experimental environment and parameters as for the next two

experiments. This experiment was conducted the 9th October 2001. The extensometer used was #0104. The test was run up to Na in one phase, without any interruption.

The second experiment I32I02 was started on the 13th December 2001 and stopped on the 21th December 2001, at the shut-down of the accelerator. The specimen was tested *in-beam*. The experiment could not be finished but reached a number of cycles larger than the one obtained in the zero-test. The experiment was run in 8 different phases, interrupted by normal beam interruptions, beam line cooling system failures, accelerator source failures, monitor failure etc... The extensometer used was again #0104. The history of experiment I32I02 is given in Fig. 3. Fifty minutes were necessary to adjust the correct beam size and position which caused 33,000 μAs of static irradiation. During the shutdown, the control baraque of the irradiation facility had to be moved to another location in the hall. This complex operation introduced some electrical problems affecting mainly the vertical drive mechanism of the irradiation head (see Fig.1).

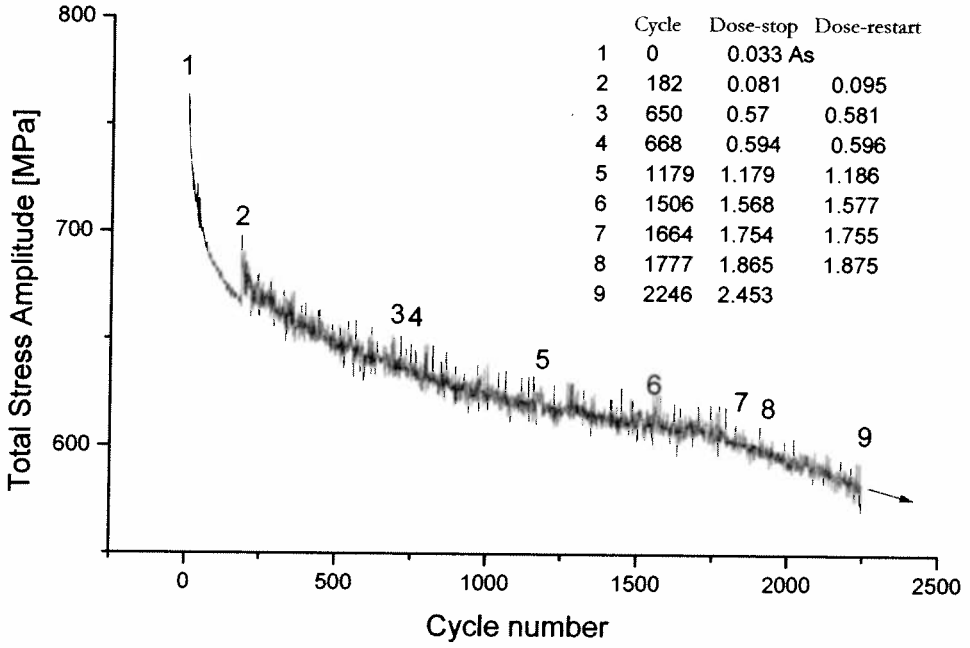

Figure 3: *History of experiment I32I02. The cyclic stress as a function of cycle number is shown and the different experimental phases are indicated with their doses at stop and restart.*

The problem was very difficult to solve. It needed many days of repair, working in the opened irradiation site. Finally the drive control system was repaired but the experiment could not be restarted, because the specimen had been stressed to unknown levels during the operation. Figure 4 indicates how the temperature is adjusted, at the beginning of the experiment. The temperature increase produced by the beam heating is shown to be around 50°C. The glued thermocouple could not survive more than 200 cycles. But this was not a problem, since the adjusted helium loop and beam parameters were hold constant up to the end. Figure 4 indicates also that the specimen was cycled without beam for 142 cycles. This mistake occurred

during night and was not announced because of a failure of the surveillance system. Nevertheless, considering the whole experiment, a duty ratio of about 0.93 was obtained (Beam time divided by mechanical time). This is not bad if compared with the first experiments done with the *in-situ* machine [13].
The last experiment I32I04 started on 28th November 2002 and ended on 4th December 2002. The aim of this experiment was to produce the post-irradiation result to compare with the *in-beam* test. The extensometer used was #0105. The first cycles of experiments I32I01 and I32I04 are shown in Figure 5, to prove for the good quality of the measuring system, since the extensometers were different in both experiments.
The history of experiment I32I04 is given in Figure 6. At beginning of experiment I32I04, 10 cycles had to be done in order to check the vacuum tightness of the specimen. The preceding experiment (I32I03) had caused the loss of one week due a problem of vacuum after a few cycles.
After those first cycles, some basic testing was conducted to check some questions related to the physical mechanisms of importance occurring during *in-beam* fatigue. The fatigue was first run without beam to the point where the hysteresis loops were relatively stable, then the beam was switched on. The test frequency was then lowered in two different steps, allowing enough time to reach stable hyteresis loops for measuring the mechanical parameters. Then the beam was switched off but the fatigue was going on a few more cycles, to detect directly the effects of the absence of beam. The justification for this testing which used 65 cycles, is given in the discussion part. The stress history of this first part of the experiment is given in Figure 6.

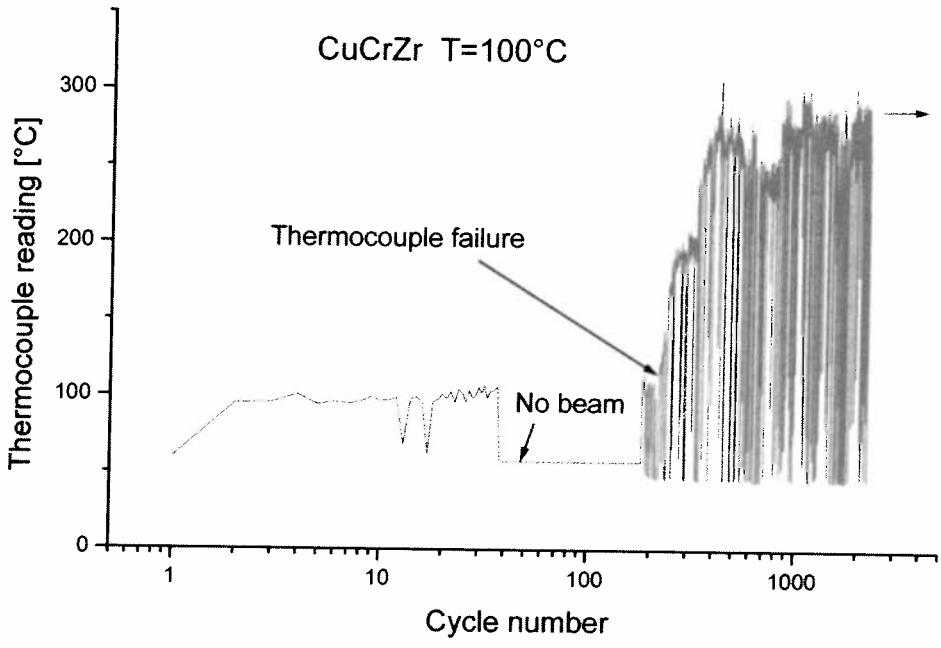

Figure 4: *Temperature history at beginning of experiment I32I02*

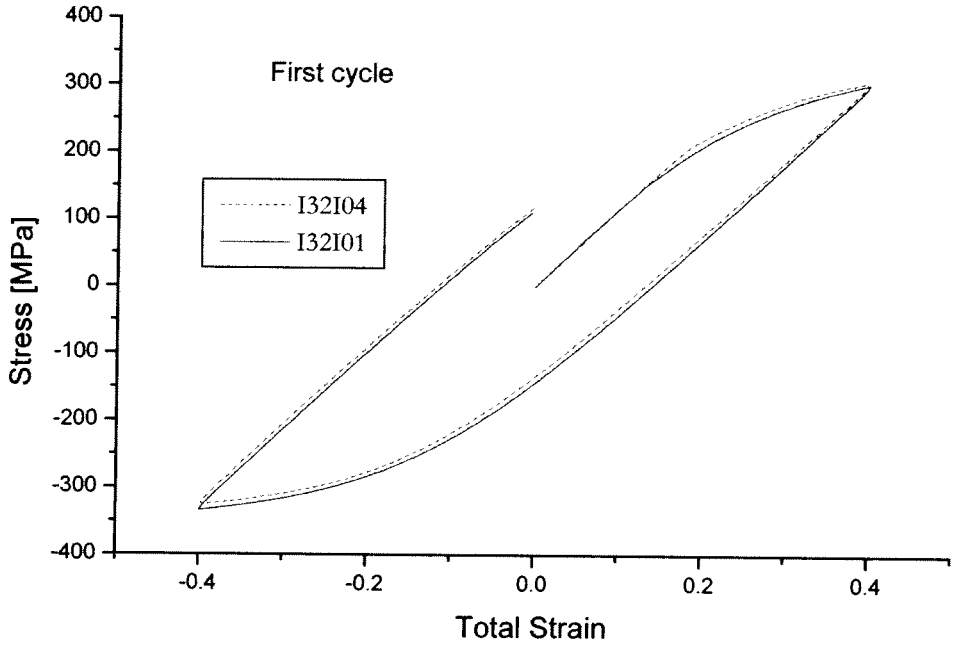

Figure 5: *Comparison of the first cycles of experiments I32I01 and I32I04*

After those 75 cycles, the specimen was irradiated statically, in order to reach a dose close to the one obtained in the in-beam test. Unfortunately the irradiation was stopped due to other beam users but it nevertheless reached a dose comparable to the targeted one (1.521 for 2.453 As). The actual doses are indicated in paragraph 6.2. The post-irradiation test was done in one phase until it reached Na, the failure of the vacuum, indicating that the first crack was through. Then the test resumed at 40°C up to total failure.
The history of I32I04 is shown in Figure 7.

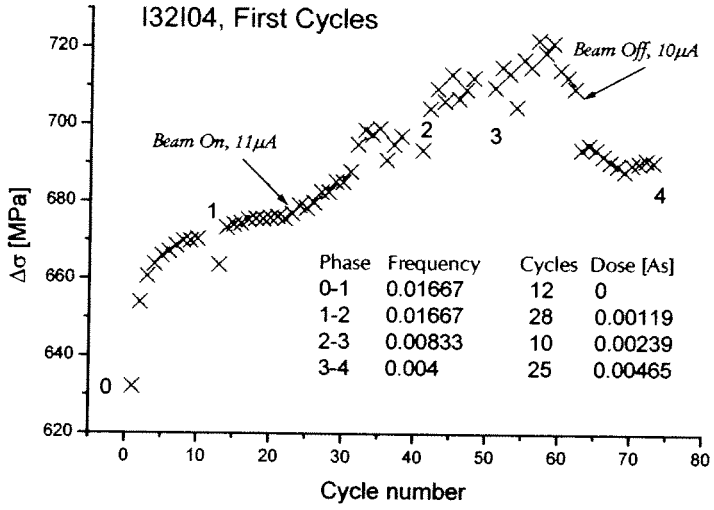

Figure 6: *Description of the first cycles of experiment I32I04. After some cycles, the beam is switched on and the frequency is changed two times. The beam is switched off again and the fatigue proceeds.*

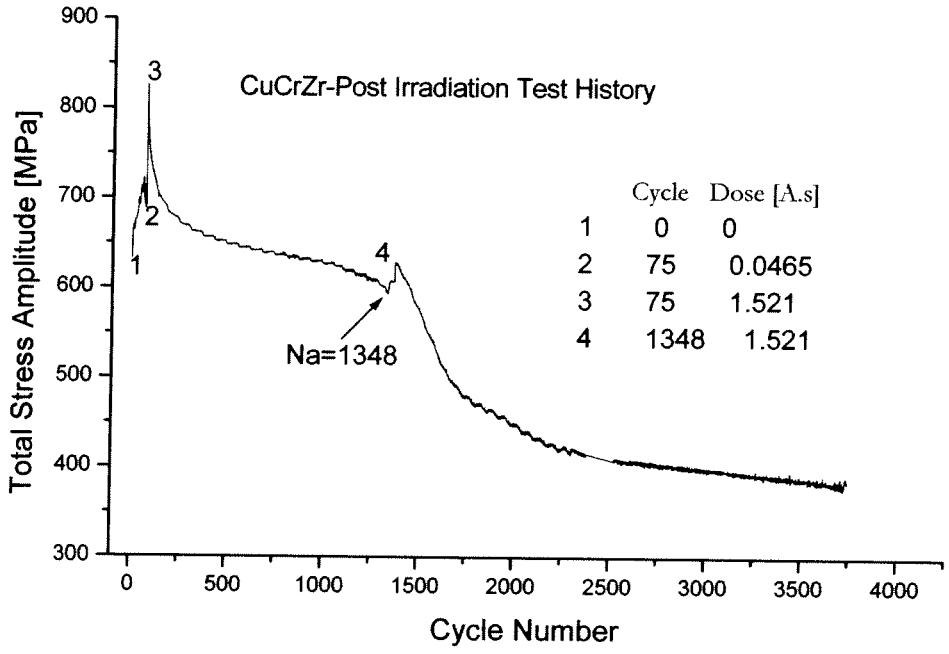

Figure 7*: Stress history of I32I04. The first phase 1-2 (75 cycles) was dedicated to the study of some physical mechanisms (see Figure 6).*

6. Results

6.1 Mechanical testing

6.1.1 General behaviour

The total stress $\Delta\sigma$ as a function of the number of cycles is represented in Figure 8, in a linear scale, for the three different experiments. The number of cycles to failure Na is indicated by an arrow. As explained before, the in–beam experiment I32I01 was interrupted before failure at N= 2246 cycles . Nevertheless it shows the longest life as compared to the zero-test I32I01 (Na=2006) and the post-irradiated test I32I04 (Na=1348). The post-irradiation tested specimen has the lowest life. The number of cycles to failure Nf (specimen separation in two parts) has not been determined. The criteria Nf is not helpful in this case, because the crack growth rate after Na in experiment I32I04 was very low, due to a particular crack orientation. The softening rate is the highest in the post-irradiation tested specimen and the lowest in the unirradiated test.

Figure 9 shows the total stress $\Delta\sigma$ as a function of the number of cycles in logarithmic scale. As explained in the preceding section, I32I02 was irradiated for 50 minutes to adjust the beam (Figure 3) and received a dose of 0.0033 As. This the reason why the stress is above the stress of experiments I32I01 and I32I04, at beginning of test. Correspondingly, in Figure 10, the total plastic strain of I32I02 is slightly below the plastic strain of I32I01 and I32I04.

I32I04 is irradiated before start of test to 1.521 As. The static hardening obtained at 0.4% total strain is not significantly higher as compared to what is obtained from I32I02. It is interesting to compare the first hysteresis loop of I32I02 and the first post-irradiation hysteresis loop of I32I04. This is shown in Figure 11. There we see that the two irradiation doses introduce a big difference in terms of plasticity. It is also interesting to note that no yield point phenomena occurs after irradiation, at a strain amplitude of 0.4%, at a test temperature of 100 °C.

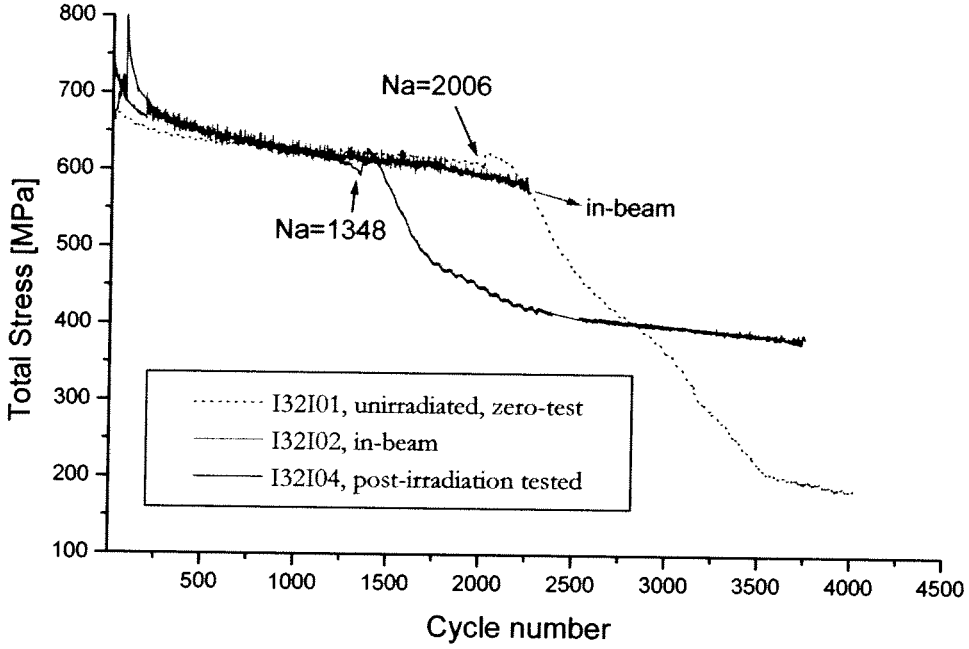

Figure 8: *Total stress as a function of the number of cycles for experiments I31I01, I32I02 and I32I04. Linear scale.*

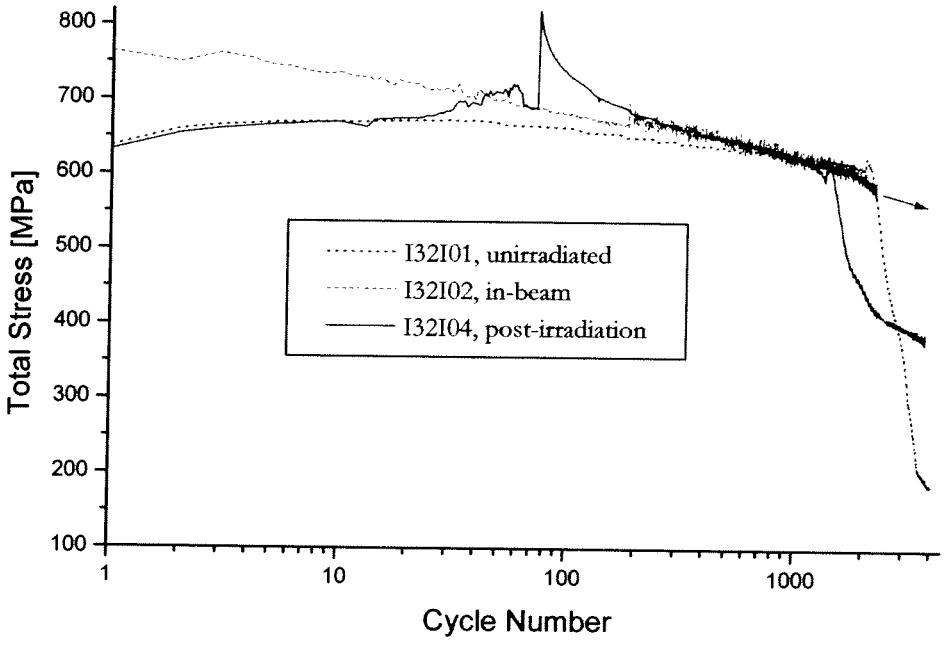

Figure 9: *Total stress as a function of the number of cycles for experiments I31I01, I32I02 and I32I04*

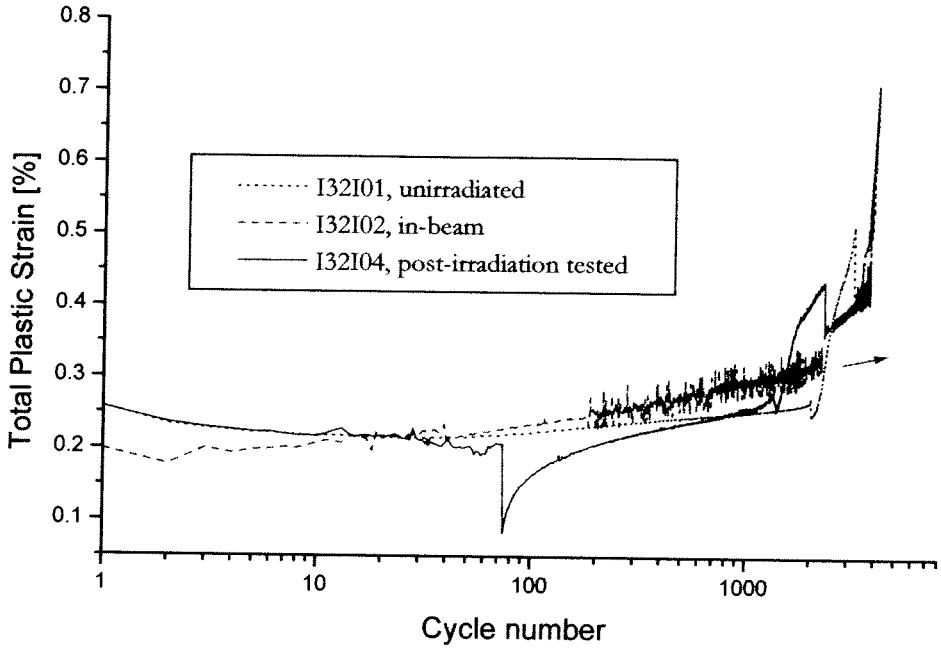

Figure 10: *Total plastic strain as a function of the number of cycles for experiments I31I01, I32I02 and I32I04*

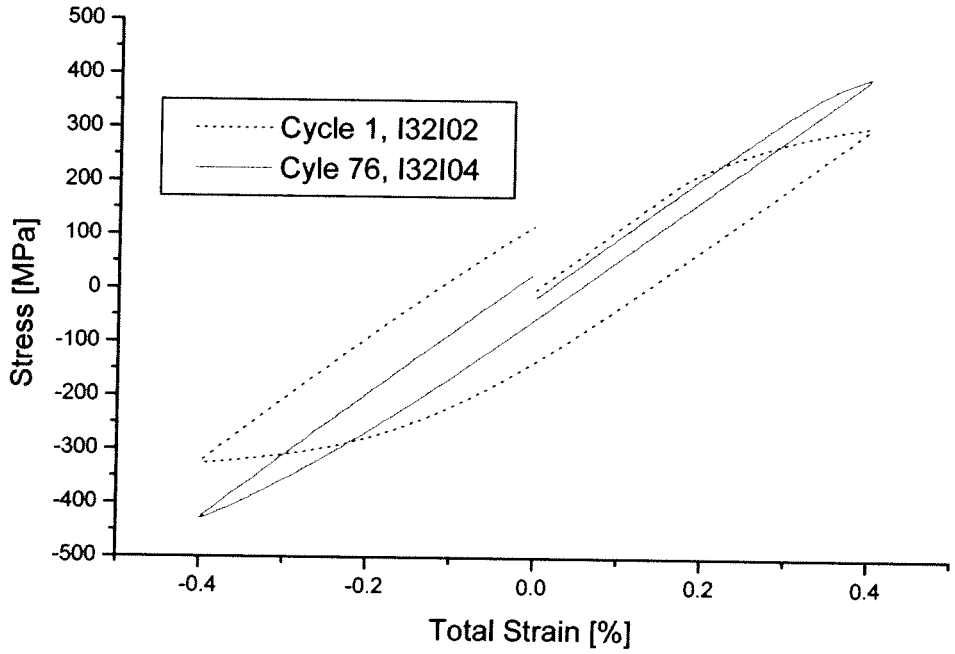

Figure 11*: First hysteresis loops of experiments I32I02 and I32I04*

6.1.2 I32I04 preliminary test

The beginning of experiment I32I04 was dedicated to the measurement of the flow stress under simultaneous irradiation in the proton beam. The idea was to establish stable conditions for the fatigue cycle, then to switch the beam on and measure the immediate effect on the flow stress. The experiment was repeated at two different strain rates to receive information about the influence of dislocation mean velocity on the flow stress under simultaneous irradiation.
The first ten cycles were done to check the vacuum integrity of the system. 65 cycles were used to realize the preliminary experiment. During those cycles it was tried to keep the temperature as stable as possible. The temperature under irradiation is the sum of the helium temperature and the beam heating temperature gradient. The accelerator was quite stable during the experiment, nevertheless some little changes may have influenced the beam shape. The beam intensity was between 11 and 10 μA. The helium temperature was set a little bit too high at the beginning of test. As a result, the temperature was higher than the targeted 100°C, at beginning of test, as shown in Figure 12.

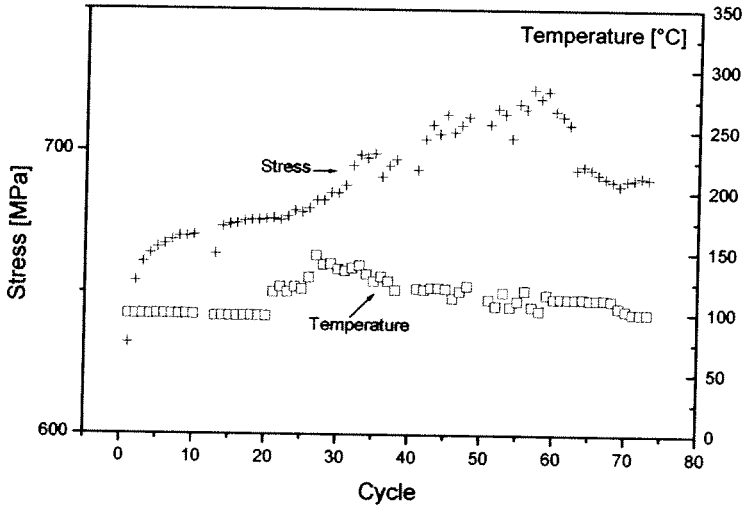

Figure 12: *The specimen temperature and the total stress as a function of the cycle number*

As shown in Figure 6, the test was run in 4 different mechanical phases. In every phase the mechanical parameters of the fatigue test are constant and the data are registered until the machine is stopped. The beam is switched on and out as indicated

in Figure 13. There, five domains with different conditions are delimited, to separate the intervals with beam on and off. Figure 13 indicates that both the proton beam and the test frequency have an immediate influence on the flow stress. The total stress (twice the flow stress) is increasing when the beam is switched on. The total stress also increases when the frequency is reduced. Accordingly, the total plastic strain diminishes as the total stress increases. In Table 5, we indicate the mean values of the total stress and of the plastic strain for each one of the five intervals. For the first interval, only the last data when the specimen reaches quasi stability, are taken into account.

Domain	BEAM	Period T [s]	Mean $\Delta\sigma$ [Mpa]	Mean $\Delta\varepsilon_{plast}$ [%]
I	Off	60	675.734	0.2174
II	On	60	688.890	0.2112
III	On	120	708.714	0.2027
IV	On	250	714.874	0.1962
V	Off	250	691.244	0.2059

Tabelle 5: *The total plastic strain and the total stress in the five different domains at the beginning of experiment I32I04.*

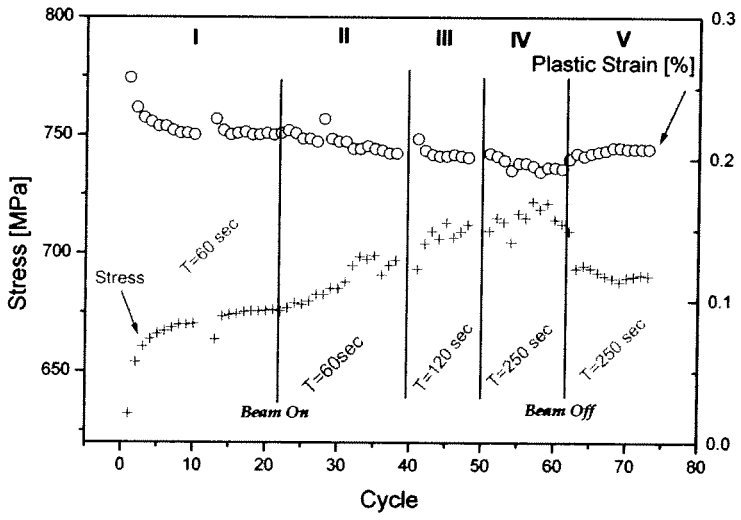

Figure 13: *The total plastic strain and the total stress as a function of the cycle number. Five domains are delimited with or without beam and different cycling periods T.*

6.2 Proton dosimetry

The radio-nuclides present into small segments from specimens I32I02 and I32I04 have been identified and the corresponding activity has been counted. Two nuclides

coming uniquely from copper have been analysed, Mn54 and Co57, in order to avoid complications from the lower mass element Cr. It is assumed that the contribution in the production of Mn54 and Co57 from Zr is negligible, because its mass is much higher and its concentration in the alloy only 0.13% (Table 1).
The production cross sections from 590 MeV protons of those nuclides are taken from the book Landolt-Börnstein, Numerical Data and Functional Relationships in Science and Technology.

For Mn54 the production cross-section is: 21.7 mb
For Co57 the production cross-section is: 25.7 mb

The fluences obtained from the Mn54 activity were 2% higher than the fluences obtained from the Co57 activity. The mean of the values is indicated in the results table below.
From the proton fluences calculated with the cross-sections indicated above, a displacement dose can be estimated based on a modified Kinchin-Pease model. A dpa cross-section is derived from the following relation:

$$\sigma_{dpa} = 0.8\frac{\delta_{E_d}}{2E_T}$$

For copper, the damage energy cross section δ_{E_D} has an accepted value of 316 barn keV and the displacement threshold energy E_T is given at 25 eV. The above cross-section is then evaluated to 5056 barn.

The results of the dosimetry are compared to those obtained from the beam time integral in the Table below. Taking into account the usual beam dispersion, the results below can be regarded as good. The dosimetry results reflect the actual dose received by the specimens.

	Beam time integral		Dosimetry	
	Fluence[p/cm^2]	Dose [dpa]	Fluence[p/cm^2]	Dose [dpa]
I32102	6.69E19	0.334	4.5E19	**0.228**
I32104	4.15E19	0.211	2.21E19	**0.112**

Table 6: *Specimens doses estimated from the beam time integral and from the dosimetry*

7. Discussion of results

The different conditions imposed to the specimens, unirradiated, in-beam and post-irradiation tested have a clear effect on the fatigue endurance of the material. The in-beam specimen has the longest life. The in-beam specimen lasts longer than the unirradiated specimen and significantly longer than the post-irradiation

tested specimen. This result is in contradiction with what has been previously measured in the case of the ferritic-martensitic steels, where the in-beam endurance was generally shorter for all cases. In fact, the response of the copper alloy is strange because despite the fact that the stress level in-situ was slightly higher, in particular at the beginning of the test (see Fig. 8 and 9), the crack growth rate is lower than in the unirradiated material. Also interesting to note is the higher softening rate in the case of the in-beam specimen (see Fig. 8). The stronger softening rate is also clearly visible in Fig. 10. The plastic component of the strain as well as the rate of increase of the plastic strain are larger in the in-beam specimen. The post-irradiation tested specimen has also a very high rate of plastic strain increase but the amount of plasticity is smaller. Only at test end, the plasticity in the post-irradiation tested specimen is larger than in the in-situ specimen. The general behavior in terms of total plastic strain and stress observed in the three specimens, seems consistent with the measured lives.

One critical aspect of this study is the fact that only one experiment is conducted per condition and knowing the dispersion which normally affects fatigue results, the results presented here could be different with a larger number of specimens. This objection is not correct because of the geometry of the specimen and the strain applied. Since the tests are conducted at high total strains (0.8%), we can assume that the time to generate a crack will be small and most of the fatigue life will be crack propagation. Therefore the scatter which usually comes from the crack nucleation period is small in our case. On the other hand, once the crack is generated, it has to run a short distance, the wall thickness of the tube specimen (450 microns), to produce the failure. Therefore the scatter is probably much smaller as compared to the scatter from bulk specimens where the crack goes long distances, can change its propagation direction, be arrested or react with other cracks. For theses reasons it is believed that the scatter, for the parameters of this experiment, is low and that the lives measured from single experiments, represent well the general behavior.

Not much information is available from the literature to compare to our results. Gorynin et al. report some results from bending tests on specimen irradiated at 90°C to 10^{21} n/cm^2 in SM-2. The authors report an increase of life at a test temperature of 300°C, after irradiation, specially at low strains. These results cannot be compared to ours, because the test procedure is very different and the heat treatments of the CuCrZr are not described [14].

Another work from Singh et al. [4, 15] gives some results on the irradiated fatigue life and deformed microstructure of copper alloys. At an irradiation temperature of 100°C to 1.5×10^{20} n/cm^2 (0.3 dpa) , prime aged (the same heat treatment as in this work) CuCrZr specimens tested at 100°C did not indicate any deleterious effects from the irradiation. But this result is an unvalid comparison to this work done at high strain, because the unirradiated strain controlled specimens are compared to stress controlled specimens. Specially at high strains, strain localizations effects could have affected the behavior of the stress controlled fatigue specimens.

A more recent work from Singh et al. [16] allows a more reliable comparison. Results from strain controlled specimens tested and irradiated at 250°C to a neutron fluence of 1.5×10^{20} n/cm^2 , are presented. At an imposed strain $\Delta\varepsilon_{tot}$ of 0.8%, the fatigue life of the irradiated specimen is reduced by approximately 20 to 30% . The number of cycles to failure lies around 2000 cycles, which is similar to the results shown in Figure 8. At higher imposed strains, the effect of the

irradiation is even stronger. The general behavior shown supports the results presented in this work.
Nevertheless it is important to note that the preliminary deformation imposed to the post-irradiation tested specimen (see Fig. 6) was probably deleterious to the fatigue endurance. The pre-deformation imposed to the specimen has probably contributed to form dislocation denuded zones and start re-arrange the dislocations into cells [15]. In such a case we can expect the formation of more stable defects and stronger barriers for the glissile dislocations, during the static irradiation. This had probably an adverse effect on the crack propagation. As explained below, the pre-deformation experiment was necessary to sort between possible physical embrittlement mechanisms.

Taking as a fact the improvement of the endurance in the in-beam case, different hypotheses can be taken into account for a tentative explanation. Some possible mechanisms which can be considered are listed and discussed below. The list is not exhaustive and represents what seems important with the knowledge available from the literature on this subject.

1. From Figure 10, we see that the plastic strain is larger in the in-beam specimen than it is in the post-irradiation tested specimen **and** in the unirradiated specimen. This fact is quite surprising. We can easily understand that it is reduced in a statically irradiated specimen. The high density of stable irradiation defects are pinning the grown-in dislocations. It is also known from other experiments [4, 15] that after irradiation, the alloy CuCrZr is prone to strain localization at temperatures around 100°C or below, and therefore suffers reduction in ductility. In this case more crack propagation rate is expected, because if the strain is localized around the crack tip, then we can expect more crack advance per cycle. The stress level is also higher in the specimen and we will get a faster crack propagation rate as predicted by a Paris law. A reduction of fatigue life after a static irradiation seems therefore logical, at least at high strains. The fact that the plastic strain is larger in the in-beam specimen (Fig.10) as compared to the unirradiated specimen, could indicate that the deformation is more homogeneously distributed during in-beam fatigue. More plastic strain could indicate that less strain localization occurs and therefore explain the life improvement. The reason why the deformation is more homogeneous in the in-beam specimen as compared to the unirradiated specimen could be due to a different dislocation structure evolution. May be because the structure formed under in-situ conditions is less prone to shear band activities. The reason why under in-beam fatigue, a different structure could form is not understandable at this point. The associated TEM analysis is missing to prove that such a change effectively occurs in the material.

2. We know from the literature [6, 7] that the strength of the CuCrZr alloy mainly depends from a very fine and complex precipitation consisting of two different types of Zr-riched precipitates. The particles are very small and their distribution depends strongly from the heat treatments. As shown by Ivanov et al. [17] an increase of the ageing heat treatment temperature and duration has a drastic effect on the strength and ductility. Increasing the aging temperature over 550°C results in over-aging and loss of strength. Over-aging causes a

fine dispersion of coarse precipitates and suppresses the formation of tiny precipitates responsible for mechanical strength [7]. The same mechanism probably explains the loss of strength to the level of pure copper, observed in precipitation hardened copper alloys when irradiated and tested at 400°C [14]. It is possible that under cyclic deformation and concurrent proton irradiation, the over-aging mechanism is taking place at much lower temperatures. This could be the reason for the observed increased plasticity. As explained above, this should contribute to an increase in fatigue life due to a more homogeneous deformation distribution and would explain why the in-beam condition is superior to the unirradiated condition in terms of endurance. The associated TEM analysis is missing to prove that precipitate coarsening occurs during in-beam fatigue

3. The spallation reactions produced by irradiation with 590 MeV protons produce a large spectrum of impurities, among them hydrogen and helium. The amounts produced at low doses (<10 dpa) are very low compared to the impurity levels already contained in the alloy, at the exception of helium and hydrogen. The amount of helium produced in pure copper was measured in the past [9] to a value of 102 appm/dpa. No detrimental effects of helium in copper are reported in the literature. At the dose levels reached in our experiments, it is believed that helium should have no significant influence. In the contrary, hydrogen is produced at much higher levels by the protons. Monte-Carlo calculations predict amounts of 530 appm/dpa [11]. Hydrogen is not known to have detrimental effects to the fatigue properties of copper. From a recent information (Private communication, S. Fabritsiev, 2002), there may be a possibility for hydrogen to facilitate the glide and the generation of mobile dislocations in copper. This could be a possible explanation for the increased plasticity measured in the in-beam specimen. This is the reason, why the beginning of experiment I32I04 was dedicated to an analysis of the flow stress, with and without beam. The experiment has been described with great details in section 5, Figure 6. The results are shown in Figure 12 and Table 5. When the beam is switched on, the stress becomes higher by a value of approximately 6.5 Mpa. When the frequency is lowered by a factor two, then the flow stress increases further by 10 Mpa. Lowering again the frequency a factor two increases the flow stress by another 3 Mpa. Stopping the beam decreases the stress to a level similar to what it was at the beginning of the experiment. From this experiment we can draw two necessary conditions. The first one is the proof that the dislocations interact with the moving dislocations, as it had been already deducted from previous experiments [10]. From the fact that the flow stress is increasing when the strain rate decreases, we can conclude that viscous drag is acting on the dislocations. This viscous drag is the consequence of the interaction of the dislocations with the irradiation defects. The interaction mechanism has been simulated by molecular dynamics and analytical modeling predicts interaction stresses of the order of the flow stress increase measured here [18]. The second conclusion is that hydrogen, which is generated by the protons, is not facilitating deformation in the copper alloy. Therefore hydrogen cannot by

itself, explain the increased plasticity in the in-beam specimen. Nevertheless, even if hydrogen does not reduce the apparent dislocation friction stress, an effect of hydrogen on the evolution of the deformation dislocation microstructure cannot be excluded.

4. Another possible mechanism, which could explain the increased life in the in-beam specimen, is related with the dynamic of the dislocation movements during the cycle, by analogy to a model developed by Weertmann and Green for stress controlled fatigue tests [19]. At the crack tip, the stress distribution and intensity is a function of the time. The stress stays below the yield limit during a major part of the cycle. During that time the situation is similar to a static irradiation and the defects can accumulate and pin the dislocations. In copper defect accumulation is fast and stacking fault tetrahedras are readily produced from the displacement cascades. During the half period of a cycle, the damage accumulated reaches 1.2×10^{-4} dpa. This is enough to produce a substantial quantity of SFT's which will pin the dislocations [20]. In such a case, the model predicts that the effective stress intensity factor at the crack tip is reduced. Because the crack advances only when the critical stress intensity factor is attained, the crack will propagate during a smaller fraction of the fatigue cycle and therefore the crack advance per cycle will be reduced. It is questionable if this model applies for the case of our experiments. First, our results indicate, from the absence of irradiation hardening, that the dislocations are absorbing the defects. Secondly, the plasticity is increased, not reduced. We also know that dislocation free channels are frequently formed in fcc irradiated copper, indicating that the defects are not strong obstacles. Therefore it is believed that a mechanism as described by Weertmann and Green is probably not taking place in our case. Nevertheless it could be wise to perform a deeper analysis to see how this model could be adapted to a strain controlled fatigue test.

The improvement of the fatigue life in the case of the in-beam deformation is probably due to a combination of some of the mechanisms described above. Some more experimental analysis (TEM) is required to study the evolution of the dislocation microstructure and precipitation. This will help to determine with more certainty, the reasons for the improvement of the fatigue life in CuCrZr, when fatigued under continuous irradiation.

8. Conclusions

A series of experiments have been conducted using an in-situ fatigue device to study the behavior of CuCrZr alloy under cyclic deformation and concurrent irradiation with 590 MeV protons, at 100°C. Three experiments have been realized, an unirradiated test, the in-beam fatigue test and a post-irradiation fatigue test. The dose reached at the end of the in-beam test was 0.23 dpa .The post-irradiation tested specimen was irradiated to 0.11 dpa. A series of deformation tests with and without concurrent irradiation was also realized, in order to measure the flow stress under beam. The main conclusions that can be drawn are as follows:

- The in-beam specimen reached the longest life. The post-irradiation tested specimen had the shortest life. The in-beam test condition is superior in terms of endurance.
- The total plastic strain measured in the in-beam specimen was larger than the plastic strain measured in the statically irradiated specimen ***and*** in the unirradiated specimen.
- The flow stress measured under beam, increases when the cyclic frequency decreases. The increase of the flow stress is a direct consequence of the interaction of the mobile dislocations with the irradiation defects. The nature of the interaction with the dislocations is viscous drag.
- Assuming high strain levels in the CuCrZr components and depending on the dynamic conditions at the first wall of ITER, the effect of the in-situ deformation could be beneficial for the fatigue endurance.

Acknowledgements:

Financial support from the European Community Fusion Technology Materials Program is gratefully acknowledged. We thank the Paul Scherrer Institute at Villigen/CH for its support throughout the experiments.

REFERENCES

[1] G. Kalinin and R. Matera, "Comparative analysis of copper alloys for the heat sink of plasma facing components in ITER," *Journal of Nuclear Materials*, vol. 258-263, pp. 345-350, 1998.

[2] V. Komarov and A. Labusov, "Analytical support for the divertor design," Efremov Institute JF-4B-99/1, April 2000 2000.

[3] K. D. Leedy, J. F. Stubbins, B. N. Singh, and F. A. Garner, "Fatigue behavior of copper and selected copper alloys for high heat flux applications," *Journal of Nuclear Materials*, vol. 233-237, pp. 547-552, 1996.

[4] B. N. Singh, J. F. Stubbins, and P. Toft, "Fatigue Performance of Copper and Copper Alloys before and after Irradiation with Fission Neutrons," Riso National Laboratory, Roskilde Riso-R-991(EN), May 1997 1997.

[5] B. N. Singh, D. J. Edwards, A. Horsewell, and P. Toft, "Dose Dependence of Microstructural Evolution and Mechanical Properties of Neutron Irradiated Copper and Copper Alloys," Riso National Laboratory, Roskilde Riso-R-839(EN), September 1995 1995.

[6] B. N. Singh, D. J. Edwards, M. Eldrup, and P. Toft, "Effects of heat treatments and neutron irradiation on microstructures and physical and mechanical properties of copper alloys," *Journal of Nuclear Materials*, vol. 249, pp. 1-16, 1997.

[7] U. Holzwarth, H. Stamm, M.Pisoni, A.Volcan, and R.Scholz, "The recovery of tensile properties of CuCrZr alloy after hot isostatic pressing," *Fusion Engineering and Design*, vol. 51-52, pp. 111-116, 2000.

[8] B. N. Singh and S. Tähtinen, "Final report on characterization of physical and mechanical properties of copper and copper alloys before and after irradiation," Risoe National Laboratory, Roskilde R-1276(EN), December 2001 2001.

[9] P. Marmy, M. Daum, D. Gavillet, S. Green, W. V. Green, F. Hegedues, S. Proennecke, U. Rohrer, U. Stiefel, and M. Victoria, "PIREX II- A new irradiation facility for testing fusion first wall materials," *Nuclear Instruments and Methods in Physics Research*, vol. B47, pp. 37-47, 1990.

[10] P. Marmy, "In-Beam Fatigue of a Ferritic-martensitic Steel. First Results.," *Journal of Nuclear Materials*, vol. 212-215, pp. 594-598, 1994.

[11] S. L. Green, "Calculated Radiation Damage Effects of High Energy Proton Beams," *Journal of Nuclear Materials*, vol. 126, pp. 30-37, 1984.

[12] W. E. King, K. L. Merkle, and M. Meshii, "Determination of the threshold-energy surface for copper using in-situ electrical-resistivity measurements in the high-voltage electron microscope," *Physical Review*, vol. B23, pp. 6319, 1981.

[13] P. Marmy, "In-Beam Fatigue of a Ferritic-Martensitic Steel," *Plasma Devices and Operations*, vol. 4, pp. 211-219, 1996.

[14] I. V. Gorynin, S. A. Fabritsiev, V. V. Rybin, V. A. Kasakov, A. S. Pokrovskii, V. R. Barabash, and Y. G. Prokofiyev, "Radiation-resistant properties of copper alloys intended for fusion reactor applications," *Journal of Nuclear Materials*, vol. 191-194, pp. 401-406, 1992.

[16] B. N. Singh, "Low cycle fatigue behavior of neutron irradiated copper alloys at 250 and 350°C," Riso National Laboratory, Roskilde March 2000 2000.
[17] A. D. Ivanov, A. K. Nikolaev, G. M. Kalinin, and M. E. Rodin, "Effect of heat treatments on the properties of CuCrZr alloys," *Journal of Nuclear Materials*, vol. 307-311, pp. 673-676, 2002.
[18] M. Hiratani, H. M. Zbib, and B. D. Wirth, "Interaction of glissile dilocations with perfect and truncated stacking-fault tetrahedra in irradiated metals," *Philosophical Magazine A*, vol. 82, pp. 2709-2735, 2002.
[19] J. Weertman and W. V. Green, "Fatigue Crack Growth under continuous radiation," *Journal of Nuclear Materials*, vol. 97, pp. 254-258, 1981.
[20] B. N. Singh and S. J. Zinkle, "Defect accumulation in pure fcc metals in the transient regime: a review," *Journal of Materials Science*, vol. 206, pp. 212-229, 1993.